Heat transfer within a multi-package: Assessing the impact of package design on the cooling of strawberries

Ahmad Nasser Eddine, Steven Duret, Denis Flick, Onrawee Laguerre, Ichrak Sdiri, J. Moureh

Heat transfer within a multi-package: Assessing the impact of package design on the cooling of strawberries

Ahmad Nasser eddine [a,*], Steven Duret [a], Denis Flick [b], Onrawee Laguerre [a], Ichrak Sdiri [a,c], Jean Moureh [a]

[a] *Université Paris-Saclay, INRAE, FRISE, 92761, Antony, France*
[b] *Université Paris-Saclay, INRAE, AgroParisTech, UMR SayFood, 91120, Palaiseau, France*
[c] *Arts et Métiers Institute of Technology, 75013, Paris, France*

ARTICLE INFO

ABSTRACT

Perishable horticultural products may necessitate multi-packaging for preservation. The optimized primary and secondary packaging designs allow to reduce cooling time and ensure uniform product temperature, thereby enhancing fruit quality. This study examined how the secondary package design impacts the cooling of strawberries in airtight clamshells (AC) during precooling. The AC design simulates heat transfer within Modified Atmosphere Package (MAP) where there is no direct interaction between the external cooling air and the internal environment of the clamshell. Laboratory experiments were conducted to simulate one level of a pallet, using artificial material instead of real strawberries in order to have a better control of thermophysical properties and thus to better investigate heat transfer mechanisms. The thermal performance of an existing tray design was compared to three new alternative designs. The effect of air headspace, vent holes area and inlet airflow rate on the cooling efficiency was investigated.

Experimental results revealed significant cooling heterogeneities among different AC positions, with the largest observed disparities being 1.8 h for half cooling time (HCT) and 3.7 h for seven-eight cooling time (SECT) in the current tray design. Incorporating vent holes into the current commercialized tray design demonstrated superior cooling performance, with 8% improvement of the overall average HCT. Analysis showed increasing the thickness of the air headspace above the AC increased 91% and 113% the overall average HCT and SECT, respectively. The research found that airflow distribution in a tray has a critical effect on the heat transfer between the AC walls and the surrounding air temperature. Thus, the packaging design is crucial in ensuring proper ventilation around the ACs.

The alternative designs or operating under a lower airflow rate revealed a potential to cut down on energy use for ventilation. Specifically, when the airflow rate was reduced by one-quarter, there was a remarkable 94% decrease in energy usage. However, this benefit is counterbalanced by a 100% increase in the overall average HCT, which might adversely affect the product quality. Hence, optimizing the packaging design is essential to ensure the right balance between energy efficiency and product quality.

The HCT exhibited a linear correlation with the external resistance, which is influenced by the airflow behavior, whatever the AC positions and tray designs.

Nomenclature

Cp	heat capacity of product, J.kg^{-1}.K^{-1}
CHTC	convective heat transfer coefficient, W.m^{-2}.K^{-1}
COP	Coefficient of Performance of Carnot
E	ventilation energy, W.h
G	flow rate, m^3.s^{-1}

(continued on next column)

(continued)

HCT	half cooling time, h
HI	heterogeneity index, %
m	mass of product in an AC, kg
$\dot{m}$	flow rate, m^3.s^{-1}
p	pressure, Pa
P	power, W

(continued on next page)

(continued)

R	thermal resistance, $K.W^{-1}$
s	surface area, m^2
S	total surface area of an AC, m^2
SECT	seven-eights cooling time, h
T	temperature, K
Y	dimensionless temperature
Superscripts and subscripts	
a	air
avg	average
ext	external
i	AC position
int	internal
Acronyms and abbreviations	
AC	airtight clamshell
MAP	modified atmosphere packaging
TD	tray design
TOA	total opening area
Greek letter	
ρ	density, $kg.m^{-3}$
λ	thermal conductivity, $W.m^{-1}.K^{-1}$
η	global performance coefficient of the cooling unit

1. Introduction

Precooling after harvest, the first thermal treatment in a cold chain, is an essential step in ensuring the preservation of horticultural products. This unit operation reduces rapidly the product temperature, inhibiting various physiological and microbial degradation (Zhao et al., 2016). Various precooling methods are employed in the agricultural industry, with forced-air cooling (FAC) as the widely adopted technique (Nasser Eddine et al., 2022). This method is particularly favored for highly sensitive products like strawberries (Kumar et al., 2023). Nevertheless, FAC tends to generate significant cooling heterogeneities, thus, non-uniform product temperature in a pallet (Dehghannya et al., 2010). These variations are related mainly to the airflow behavior within the package which influenced by the package design. Therefore, it underscores the significance of a ventilated package design that guarantees a rapid and uniform cooling (Pathare et al., 2012). Many studies have investigated the effect of the package design on the behavior of airflow, cooling rate and heterogeneity using experimental (Mukama et al., 2017; Ngcobo et al., 2013; Wu et al., 2018), numerical (Wu et al., 2019) or both approaches (Defraeye et al., 2013; Gruyters et al., 2019). These studies are tailored to specific products as the optimal package design is inherently product-specific (Defraeye et al., 2013). The presence of vent holes on the package plays a crucial role in regulating the distribution of airflow among the fruits, thereby exerting a significant impact on the overall cooling rate and homogeneity. Various parameters related to vent holes, such as their numbers, size, shape, positions, and the symmetry of their placement on the packaging, have been assessed for their impact on cooling efficiency (Agyeman et al., 2023; Berry et al., 2016; Dehghannya et al., 2011; Delele et al., 2013; Han et al., 2017; Wang et al., 2020; Wang et al., 2019).

Multi-packaging is vital for products with high degrees of perishability, it consists of a primary packaging (consumer sale unit) like a polyliner (O'Sullivan et al., 2016) or clamshell (Anderson et al., 2004; Ngcobo et al., 2013) and a secondary packaging such as a box or tray. In certain cases, primary packaging can act as a barrier between the cold air and the produce, which can have a notable impact on the cooling rate like in the case of kiwifruit polyliner (O'Sullivan et al., 2016), or for non ventilated primary packaging such as Modified Atmosphere Packaging (MAP). Using MAPs holds potential for preserving the quality of strawberries while mitigating the risk of anaerobic conditions and their associated undesirable effects (Rashvand et al., 2023).

Studies on the impact of MAPs on the product quality generally focused on a single unit and assumed uniform environmental conditions around the MAP (Rashvand et al., 2023). However, few studies on the impact of secondary packaging design, the positioning of MAP within the secondary packaging and the stacking pattern on the cooling

uniformity of products were undertaken. Considering these factors, it is essential to understanding the cooling process and product quality within the packaging.

The utilization of plastics in packaging has resulted in significant environmental repercussions (Delahaye et al., 2023). In order to find an alternative, a new biodegradable clamshells made from carton, designed to maintain a modified atmosphere for strawberries, has been developed in a research project. However, the impact of incorporating such packaging into trays remains unknown.

To address this gap, this study introduces a new approach by using airtight clamshell (AC) to simulate heat transfer within MAP during the precooling process. This method offers a good representation of the convective heat transfer through MAP walls, induced by airflow patterns around the MAPs with respect to their arrangement and positions within the tray. This understanding is essential for improving the shelf life of packaged products. Additionally, this study assesses how various tray designs (considered as secondary packaging) affect the forced-air cooling of strawberries packed in the developed biodegradable AC. The research delves into the influence of key factors, i.e. vent holes, headspace above the AC and inlet airflow rate, on the cooling rate and the uniformity of cooling of strawberries.

2. Materials and methods

2.1. Experimental device

In a FAC facility, pallets are often arranged in parallel rows within a cooling tunnel. This tunnel is built within a cold room. Powerful fans at one end of the tunnel pull cold air through these pallets, ensuring uniform cooling of the perishable products. The current pallet arrangement in industry is made of several layers, with four trays per layer (Fig. 1). Uniform airflow distribution can be expected between the different pallets positions and layers and this was confirmed by Mercier et al. (2019), who observed no significant difference in cooling rate whatever the positions in pallet. Therefore, in our experimental device, a half layer of a pallet (i.e., 2 trays as shown in Fig. 1) was studied, assuming no heat exchange between the trays (horizontally and vertically) and between the trays and the exterior domain (air). This assumption may not hold true in real-world scenarios, especially during other stages of the cold chain, such as transport and supermarket cold room.

The experimental device, representing an air tunnel, was placed inside a temperature controlled room. It is a rectangular duct of three sections: an inlet section (600 mm length), a middle section containing two plexiglass trays (2×380 mm length), and an outlet section (300 mm
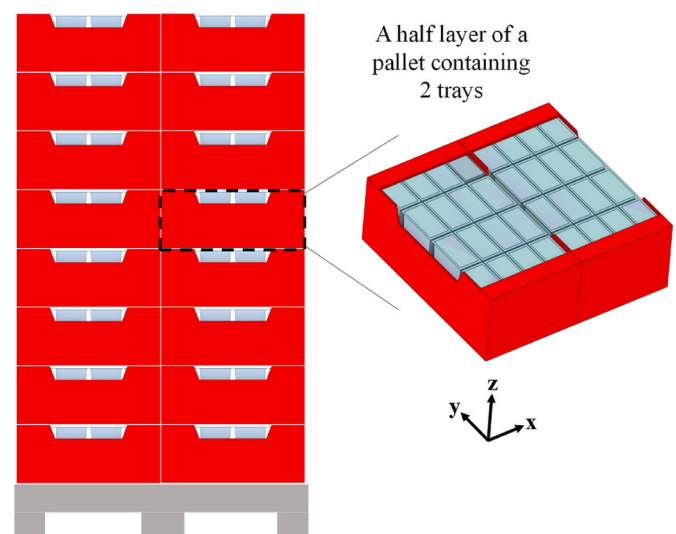

Fig. 1. Pallet with 4 trays in each layer.

length) as depicted in Fig. 2a. Two axial fans (called FAC fans in the rest of the manuscript) were installed at the outlet section to create a pressure differential between the inlet and outlet, enabling airflow through the trays. These fans, model RS PRO 24 V DC, have an airflow rate of 33.6 l s^{-1}, a static pressure of 22.4 Pa, a fan speed of 1800 RPM, and dimensions of 120 mm by 120 mm by 25 mm. The power supplied to these fans was carefully regulated to maintain the desired airflow rate at the tunnel entrance. A honeycomb was placed at the tunnel's inlet to enhance the stabilization of airflow and promote uniform air velocities. The system was sealed to prevent air infiltration. In order to represent half of a pallet layer sandwiched between two other layers with no heat exchange between them, the top, bottom, and lateral sides of the trays were insulated by a 40 mm thick layer of polystyrene foam (not shown on Fig. 2). The dimensions of a tray are presented in Fig. 2b. In this type of tray, ventilated PET clamshells containing 250–300 g strawberries are often used in practice. Measuring the temperature of strawberries within MAP is challenging due to the need to maintain the CO_2 and O_2 concentrations inside the package. Installing too much thermocouples inside the clamshell to measure strawberries temperature can disturb this atmosphere. Therefore, we focused in our experiments exclusively on the heat transfer phenomenon, the mass transfer due to transpiration and respiration processes were not considered. In the experiments, as the precooling process is aimed, the influence of the respiration heat on heat transfer was considered negligible. This is attributed to the fact that the heat produced by the respiration of horticultural products is unlikely to significantly impact the rate of cooling, mainly because the short duration of the precooling process (Sadashive Gowda et al., 1997). According to that, each tray contained 16 ACs made of carton (cellulose) filled with strawberries (Fig. 2c and d). Using the AC approach for simulating heat transfer inside the MAP ensure that there is no direct contact between the cooling air and the strawberries inside the ACs. To maintain consistency and reproducibility in the experiments, real strawberries, known for their high perishability, were replaced with PVC strawberries of 1 mm wall thickness. These PVC strawberries were filled with a carrageenan gel mixture containing 96 % water, 3% carrageenan and 1% preservatives (including sodium benzonate). The gel's high

water content results in thermal properties close to those of real strawberries (Table 1).

Each AC was filled with 20 strawberries of 15.44 g $\pm$ 0.24 g per strawberry, thus, the total mass of an AC is 0.309 kg. The arrangement of strawberries was kept identical within each individual AC. A polyethylene transparent film was used to cover the top face of the AC.

2.2. Measurements

Due to the symmetry of the AC arrangement in a tray and the central position of the main trapezoidal vent hole, a symmetry plane has been considered only in the middle of the tray and temperature measurements were performed on half of the tray to assess the cooling behavior. Accordingly, the instrumented half tray domain is limited by a symmetry plane, where all normal fluxes and gradients are assumed to be zero (zero normal velocity "$V_y = 0$" and zero normal gradients of temperature and velocity). Therefore, the non-instrumented part of the tray is expected to exhibit similar cooling behavior to the instrumented one.

The temperature of five strawberries in the following positions AC 1-2-7-8-9-10-15-16 was recorded (highlighted in green in Fig. 3a), the positions of these strawberries are indicated in Fig. 3c. In the remaining ACs (i.e. AC 3-4-5-6-11-12-13-14), the temperature of only one strawberry (Straw.5 in Fig. 3c) was measured. In toal, 48 strawberries had their core temperatures recorded every 10 s using type T thermocouples (200 μm diameter) via a data logger (Keysight DAQ970A) and

Table 1
Thermophysical properties of real strawberries and carrageenan gel.

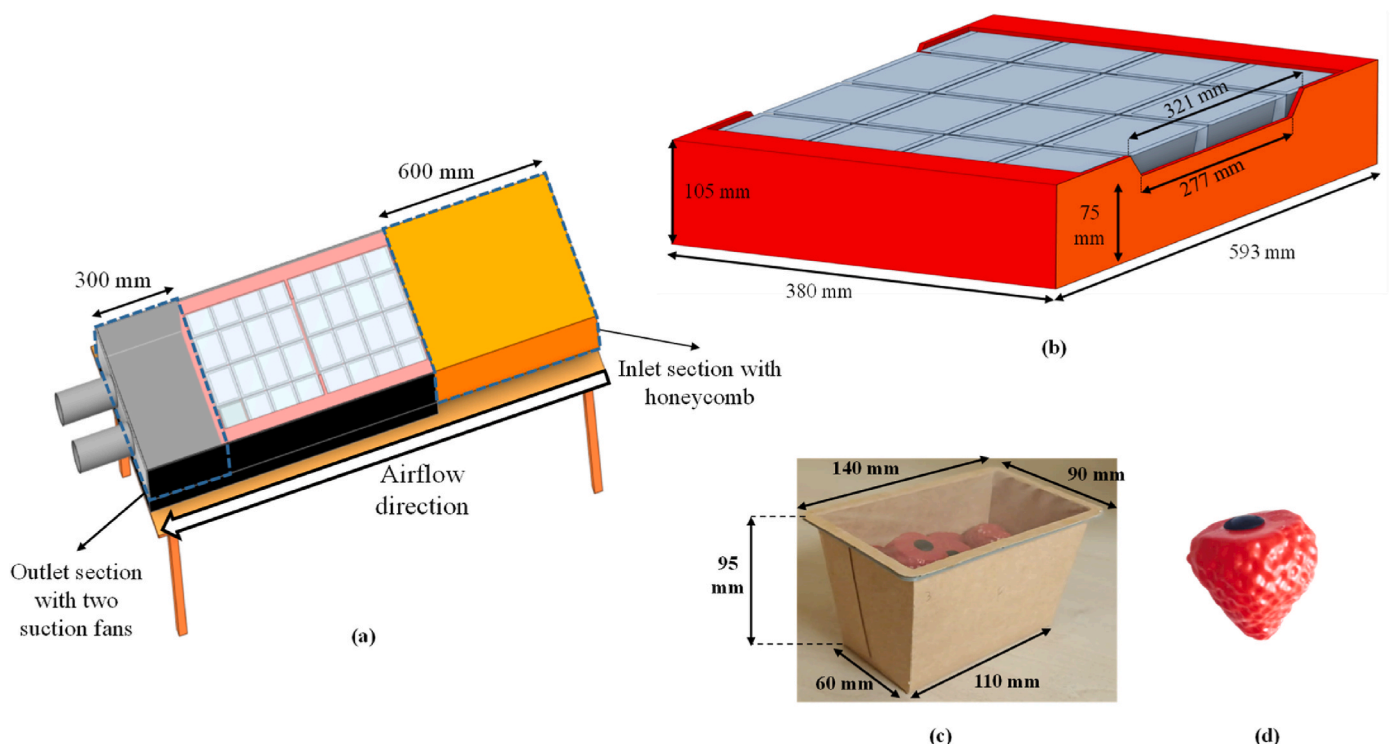| Property	Strawberries (Wang et al., 2019)	Carrageenan Gel (Agyeman et al., 2023)
λ (W.m^{-1}.K^{-1})	0.56	0.52
ρ (kg.m^{-3})	800	1013
C_p (J.kg^{-1}.K^{-1})	4000	4100

Fig. 2. a) Experimental setup, b) tray dimensions, c) filled AC dimensions, d) strawberry model.
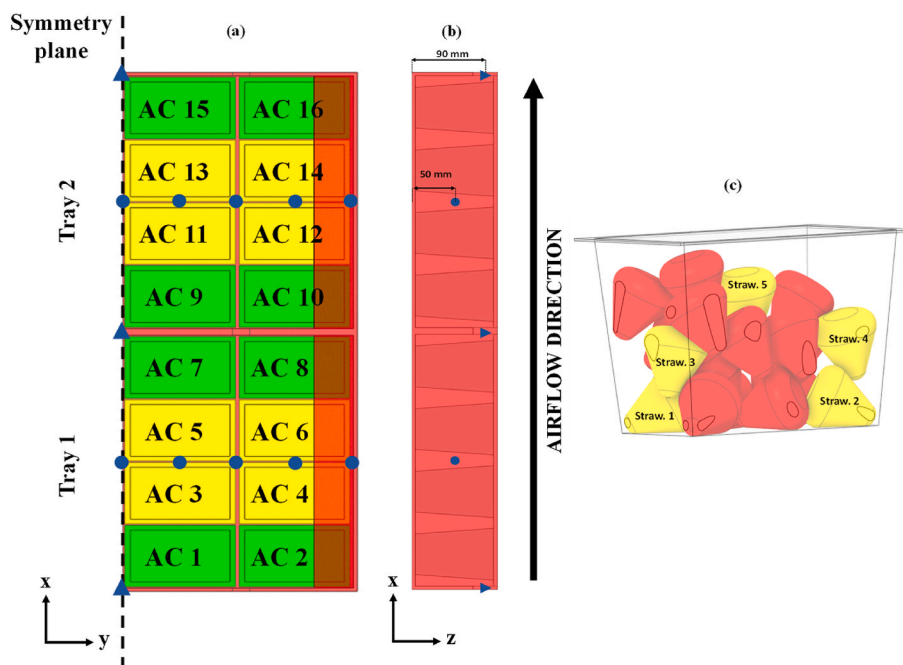
Fig. 3. a) AC positions equipped with thermocouples, green (5 instrumented strawberries), yellow (1 instrumented strawberry, straw.5), b) Thermocouple positions for air temperature measurements, c) positions of instrumented strawberries within an AC.

acquisition software (Keysight BenchVue). These thermocouples were placed in the core of the strawberries through a small orifice made in the head of the strawberry which was closed after the inclusion of the thermocouples. Given that the Biot number (Bi) is much less than 1, the core temperature is taken to represent the average temperature of the product. Additionally, air temperature was recorded using the same type of thermocouples at various locations within the trays, between the ACs (circular points in Fig. 3a and b), and at the main trapezoidal vent holes (triangular points in Fig. 3a and b). The thermocouples used were individually calibrated internally between 0 and 20 °C, with an uncertainty of ±0.1 K.

2.3. Tray designs

The performance of an existing open-top tray design currently used, referred to as TD 1, is compared to three alternative designs proposed by this study, namely TD 2, TD 3, and TD 4 (Fig. 4) to assess the impact of additional orifices and increased headspace above the ACs. TD 1 features a trapezoidal lateral orifice with a 5 mm air headspace above the AC. TD 2 is similar in size to TD 1 but incorporates four additionnal circular vent

holes (30 mm diameter) on the tray's longitudinal frontal face. In the case of TD 3 and TD 4, the tray's height has been raised to 128 mm, ensuring a larger 28 mm air headspace.

The cooling rate of product in these 4 tray designs subjected to the same airflow rate was assessed and compared. To achieve this, the air velocity at the entrance of the tunnel was carefully measured using an LDV device (Dantec FlowExplorer-2D). This measurement was essential for calculating the inlet airflow rate and ensuring the same airflow rate during the experiment of different tray designs. Knowing the cross section area of the inlet tunnel, the airflow rate was determined to be 8.9 L s^{-1}. Considering the total mass of 9.9 kg for 2 trays ($2 \times 16 \times 0.309$ kg), the resulting airflow rate per kg of fruit would be 0.9 L s^{-1}.kg^{-1}. This value of airflow rate is the same order of magnitude as the one for precooling across the pallets in industry (Berry et al., 2016).

Taking into account the variation in real use condition, pallets of freshly harvested strawberry can be transported to a FAC facility or directly transferred to a well-ventilated cold room in order to rapidly remove the field heat. Then, pallets are transferred through cold chain facilities in order to maintain the desired low temperature. This underscores the significance of studying the impact of airflow rates on the
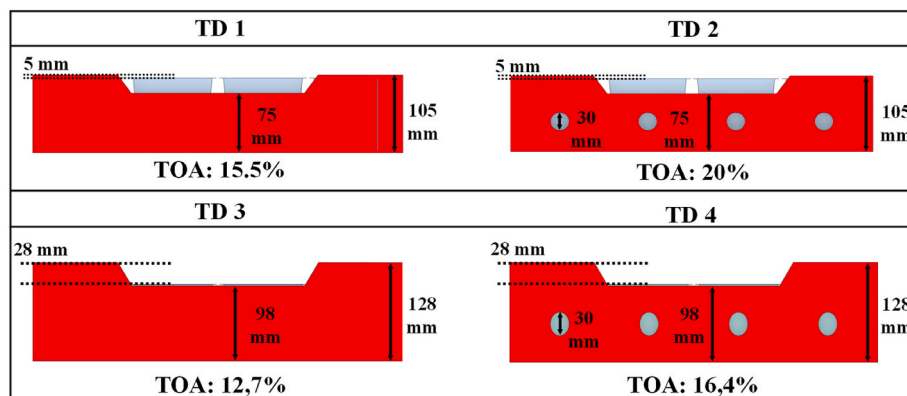

Fig. 4. Dimensions and total opening area (TOA) of 4 tray designs (TD 1, TD 2, TD 3 and TD 4).

cooling process.

In the case of TD 1 (current design), two different airflow rates were examined: $0.9 \ L.s^{-1}.kg^{-1}$ representing the high inlet velocity case (e.g. FAC facility) and $0.2 \ L.s^{-1}.kg^{-1}$ representing the low velocity case (e.g. cold room).

The pressure drop (Δp) through the 2 trays of strawberry ACs was measured using pitot tubes (7 mm diameter and 350 mm length) installed at the inlet and outlet sections of the experimental setup and connected to testo 400 universal IAQ device to record the measured value. The accuracy of the device provided by the manufacturer, for a range 0–2500 Pa, is ± 0.3 Pa + 1% value of the measured work (v.Mw.).

2.4. Experimental protocol

Five experiments were conducted, the conditions are outlined in Table 2, with two experimental trials per condition to ensure replicated data. For every experiments, the cold room was initially set to 20 °C to ensure uniform product temperatures. Subsequently, the entire experimental setup was well insulated with polystyrene foam, the fans were "off "to avoid air circulation, and the cold room temperature was lowered to 4 °C. After a 30 minutes phase of ambient temperature stabilization at 4 °C in the test room, the polystyrene foam was removed from both the inlet and outlet of the experimental setup, and the fans were "on" to start the experiment. All temperatures were continuously recorded every 10 s until temperature stability was uniformly achieved across all products, signifying that a steady state had been reached. The results presented in section 3 are the average of two repetitions.

2.5. Cooling performance parameters

Maintaining uniform cooling between individual strawberries within ACs and between the different AC positions is of paramount importance for ensuring consistent product quality and shelf life (Defraeye et al., 2015). In our study, the cooling performance can be evaluated by four factors: Convective heat transfer coefficient (CHTC), cooling times (HCT and SECT), temperature heterogeneity index (HI) and system energy consumption (E).

2.5.1. Convective heat transfer coefficient

CHTC is the rate of heat transfer between an AC wall and air per unit surface area per unit temperature difference between the wall and the air $[W.m^{-2}.K^{-1}]$. Typically, the convective heat transfer coefficient for laminar flow is relatively low compared to the one for turbulent flow. Thus, a packaging design which allows high CHTC (high ventilation around an AC), more rapid cooling could be expected. In our previous study (Nasser eddine et al., 2023), the CHTC was measured for each side of the ACs. This was done by equipping the five sides (top and four lateral sides, excluding the bottom) of one AC with heat flux sensors (30-mm diameter; Captec-France) and thermocouples. A heating resistor was integrated within the heat flux sensor in order to create a temperature difference between the cooling air and the AC surfaces. After reaching a steady state, Newton law's of cooling was used to calculate the CHTC of each side. The instrumented AC was moved to different positions to measure the corresponding CHTCs for each position. The weighted average CHTC of the five sides of an AC at position i can be estimated by eq. (1):

2.5.2. Cooling times

The dimensionless temperature (Y) defined in eq. (2), is used to normalize time-temperature evolution of product, allowing the calculation of cooling times and the comparison of the results obtained from experiments with slight difference in initial temperatures (Brosnan and Sun, 2001). In fact, it was difficult to obtain exactly the same product initial temperature in different AC positions and in different tray designs.

$$Y = \frac{T_s - T_a}{T_{s,0} - T_a} \qquad (2)$$

where T_s is the temperature of strawberry in an AC at a given time of cooling, $T_{s,0}$ is the initial temperature of strawberry, and T_a is the set ambient temperature in the test room.

Key parameters in this analysis are the HCT and SECT, which indicate the time to cool down the produce to a temperature value that is half (Y = 0.500) and seven-eighths (Y = 0.125) from the initial temperature difference between produce and cooling air (Brosnan and Sun, 2001). The SECT is of particular interest in commercial cooling operations, signifying when produce temperature is close to the required storage temperature and it can be moved to storage facilities with lower energy costs to maintain its temperature (Brosnan and Sun, 2001; Defraeye et al., 2015).

2.5.3. Heterogeneity index

HI (eq. (3)) is a valuable tool, measuring the deviation of an individual product instantaneous temperature from the average temperature of all instrumented products within an AC at a specific time.

$$HI = \frac{|T_s - \overline{T}|}{T_{s,0} - T_a} \times 100 \qquad (3)$$

Where $\overline{T}$ is the average temperature of five strawberries inside each AC, T_s is the temperature of one strawberry item in the AC. In our study, HI at the half cooling time was calculated for the 4 tray designs. The concept of HI was also used by Dehghannya et al. (2010).

2.5.4. System energy consumption

Different loads contribute to calculate the total energy consumption within a cooling facility such as (1) field heat within the produces; (2) ventilation system, such as fan within the FAC tunnel and other refrigeration components; (3) heat losses from the cooling room to the external environment; (4) air infiltration; (5) fruit's heat of respiration and (6) moisture evaporation from the fruit.

The total energy consumption within a FAC facility includes the energy consumption of the compressor, fans, and other components (evaporator, condenser, pumps, control device). The main contributor to the total heat load during cooling is the field heat of horticultural products. Since the same strawberry mass is used in each tray design given that each pallet carries the same total fruit weight, thus the average compressor power (P_{comp}, W) varies with the package design due to differences in cooling time as shown in equation (4).

$$P_{comp} = \frac{m \times Cp \times \Delta T}{SECT_{max} \times \eta} \qquad (4)$$

Where m is the total mass of strawberries (kg), Cp $(J.kg^{-1}.K^{-1})$ is the heat capacity of strawberries, ΔT (K) is the temperature difference between the initial temperature of strawberries and the one at the SECT

$$CHTC_{avg.i} = \frac{(CHTC_{right.i} \times s_{right}) + (CHTC_{back.i} \times s_{back}) + (CHTC_{left.i} \times s_{Left}) + (CHTC_{front.i} \times s_{front}) + (CHTC_{top.i} \times s_{top})}{s_{right} + s_{back} + s_{Left} + s_{front} + s_{top}} \qquad (1)$$

Table 2
Conditions of the tested configurations.

Packaging design	TD 1 (case 1)	TD 2	TD 3	TD 4	TD 1 (case 2)
Airflow rate per unit of fruit mass (L.s^{-1}.kg^{-1})	0.9	0.9	0.9	0.9	0.2
Average pressure drop Δp (Pa) ± measurement uncertainty	10.5 ±0.4	7.0 ±0.4	2.4 ±0.3	1.8 ±0.3	1.2 ±0.3

(6 °C in our case), COP is the coefficient of performance of Carnot, and η is the global performance of the cooling unit.

The energy consumption of the compressor remains the same across different designs. Therefore, opportunities to reduce energy consumption lie in optimizing the ventilation system (FAC fans) and other refrigeration components. Using an efficient tray design will lead to decrease the cooling time and the pressure drop across the pallets which will have an impact on the energy consumption of these components.

In this study, only the ventilation energy consumption (E$_{FAC\ fan}$) was calculated taking into account only the two installed fans. To estimate E$_{FAC\ fan}$ (W.h), the highest value of SECT$_{max}$ (h) of each design was used and eq. (5) was applied:

$$E_{FAC\ fan} = P \times SECT_{max} \quad (5)$$

Where P$_{FAC\ fan}$ (W) is the demand power estimated from the product of the pressure drop Δp (Pa) and flow rate across the pallet layer ($\dot{m}$, m^3.s^{-1}) (eq. (6)) (Han et al., 2018).

$$P_{FAC\ fan} = \Delta p \times \dot{m} \quad (6)$$

2.6. Statistical analysis

One-way variance analysis (ANOVA), followed by a Tukey's HSD test, were conducted to assess the significance of average temperature differences between various AC positions within trays at average HCT. This analysis allows to evaluate if the effect of different tray designs and airflow rates on HCT and SECT is statistical significant with a critical p-value of 0.05 (p ≤ 0.05).
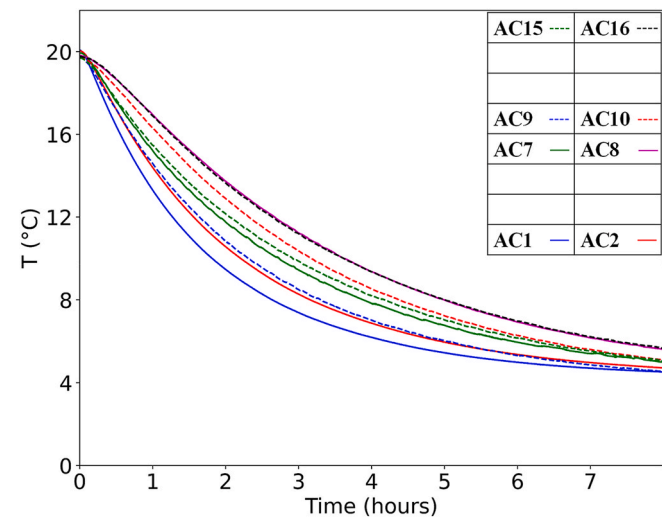

Fig. 5. Evolution of strawberries average temperature inside different ACs equipped with five thermocouples: ACs 1, 2, 7 and 8: solid blue, red, green and magenta lines, respectively; ACs 9, 10, 15 and 16: dashed blue, red, green and magenta lines, respectively.

3. Results and discussion

3.1. Reference case: TD 1

The temperature profiles displayed in Fig. 5 depict the average temperature of the five strawberries in ACs1, 2, 7, 8, 9, 10, 15 and 16 during a cooling from 20 °C to 4 °C for the configuration TD 1 (airflow rate = 0.9 L s^{-1}.kg^{-1}).

The results indicate a significant disparity in cooling rates among the different AC locations, with AC1 cooling the fastest and ACs 8 and 16 cooling the slowest. There is a statistically significant difference (p < 0.05) in average temperature between AC1 and both AC8 and AC16. The cooling behavior of each AC within a tray is primarily influenced by the convective heat transfer coefficient at the AC walls (Nasser eddine et al., 2023) and the air temperature. Both of these two parameters are affected by the airflow pattern, which, in turn, is determined by the package design. As seen in Fig. 6, the air in the pathway at tray's edge (positions 5 and 10) warmed up more than the air in the headspace (inlet, middle and outlet orifices). The air temperature heterogeneity is more pronounced at the beginning of the cooling process, the difference between the air temperature at the inlet orifice of tray 1 and air at position 10 (at the edge of tray 2) reaches 10 °C at 15 min (Fig. 6). This difference gradually diminishes to 4 °C at the average half cooling time of 137 min. Consequently, two types of cooling heterogeneity can be identified. The first one is along the central part of the tray which is highly ventilated by forced-convection mechanism through the main airflow, as evidenced by the AC1 and AC9 having nearly the same and highest heat transfer coefficient (CHTC$_{avg.1}$ = 31 W m^{-2}.K^{-1}, CHTC$_{avg.9}$ = 35 W m^{-2}.K^{-1}) (Nasser eddine et al., 2023) and small temperature difference between middle and inlet orifices.

A noteworthy observation, although not statistically significant (p > 0.05), was that the strawberries inside AC9 cool faster than within AC7 (Fig. 5). This result can be explained by the predicted airflow behavior in the packaging system. Upon exiting Tray 1, the mixing of cold air from the headspace and warm air coming from the pathways around the vertical walls of ACs occurred. This mixing, coupled with the lower heat transfer coefficient of AC7 compared to AC9 (CHTC$_{avg.7}$ = 27 W m^{-2}.K^{-1}, CHTC$_{avg.9}$ = 35 W m^{-2}.K^{-1}), explained the faster cooling of fruits in AC9. This phenomenon was also observed by Ferrua and Singh (2009).

The second significant heterogeneity is observed in the width of the tray, between pairs such as AC1 and AC2, AC7 and AC8, AC9 and AC10, and AC15 and AC16. The ACs located near the lateral tray wall are not exposed to the main airflow but to weaker secondary air streams generated by entrainment and diffusion mechanisms. This leads to locally higher temperatures as in AC8 and AC16. These ACs had the lowest cooling rate due to their location in less ventilated areas and exposition to warmer air as it traveled in almost stagnant areas between the ACs before reaching these positions.

3.2. Effect of tray design on cooling rate and heterogeneity

The comparison of cooling performance among different tray designs is presented in Fig. 7 using the average HCT and SECT of five strawberries within ACs1, 2, 7, 8, 9, 10, 15, 16. Additionally, Fig. 8 presents air temperatures at different positions at 137 min, corresponding to the average HCT of the reference case TD 1 (airflow rate = 0.9 L s^{-1}.kg^{-1}). In the case of TD 1, AC16 exhibits significantly longer HCT and SECT, at 2.7 h and 7.4 h, respectively, compared to AC1, which has HCT and SECT values of 1.3 h and 4.0 h.

As it can be seen on Fig. 7, adding circular vent holes (TD 2) and working with the same airflow rate as TD 1 yield a slightly improved cooling rate compared to TD 1, though the differences in HCT and SECT were not statistically significant. Particularly, AC2 showed a 21% reduction in HCT and a 10% in SECT, AC8 exhibited a 23% reduction in HCT and a 12% reduction in SECT, and AC10 demonstrated an 18% reduction in HCT and a 7% reduction in SECT. These ACs benefit from
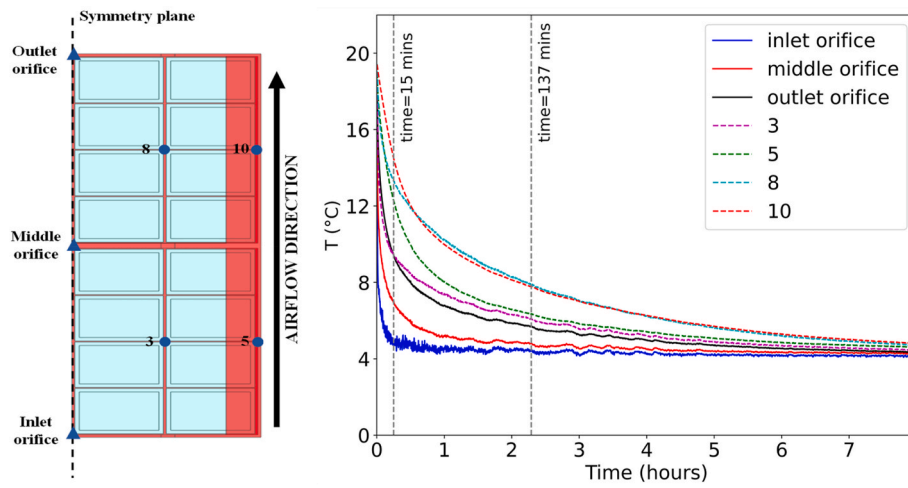
Fig. 6. Evolution of air temperature within TD 1 (airflow rate = 0.9 L s^{-1}.kg^{-1}).

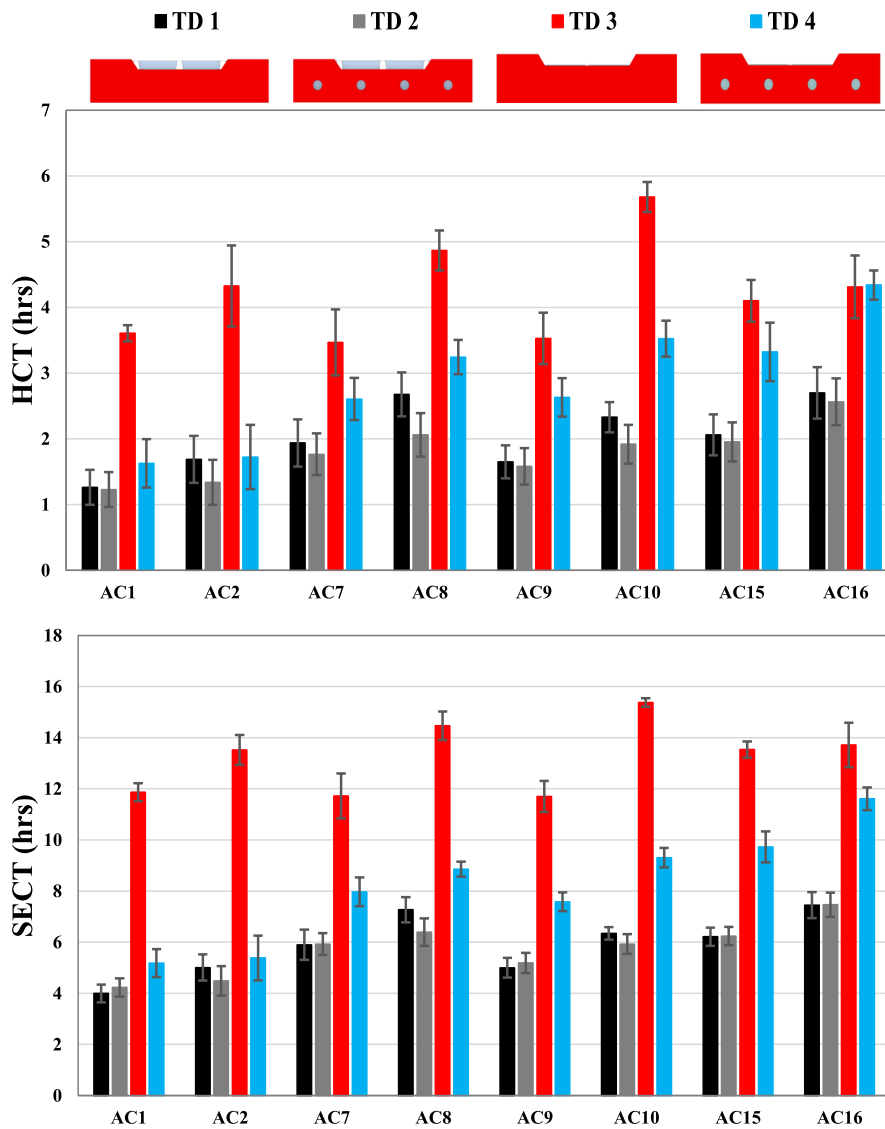**Fig. 7.** Experimental cooling times HCT and SECT (hrs) for different tray designs (airflow rate: 0.9 L s^{-1}.kg^{-1}), error bars present the standard deviation of the 5 strawberries.
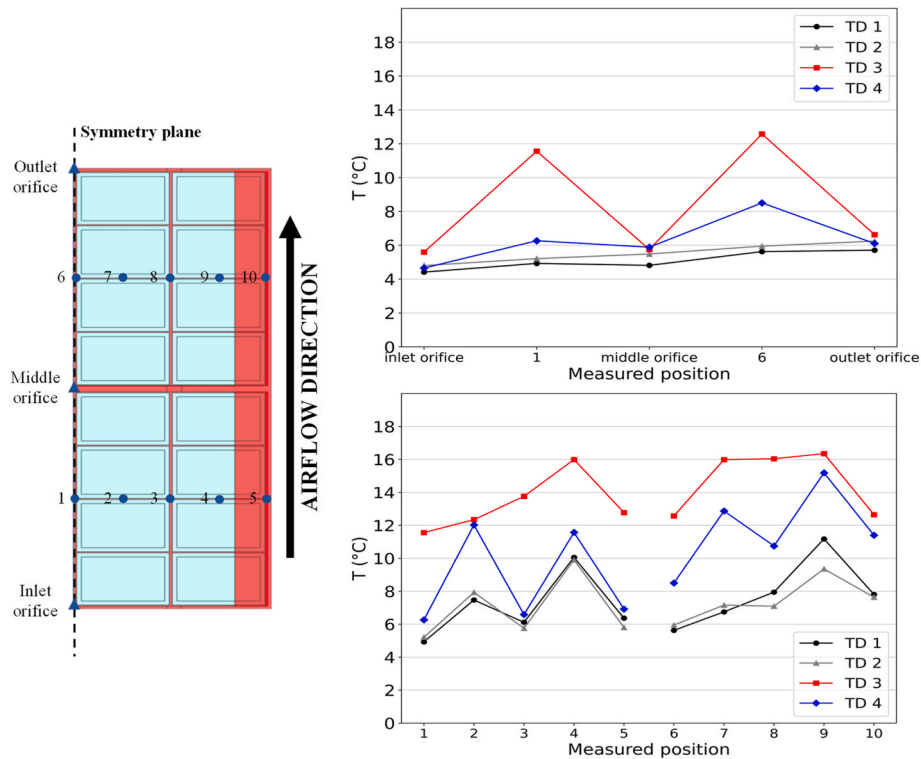
Fig. 8. Air temperature recordings from various positions within the two trays, measured after 137 min of cooling, across four tray designs: TD 1, TD 2, TD 3, and TD 4.

enhanced airflow due to their position in front of the added vent holes. Fig. 8 indicates that these added vent holes have minimal effect on air temperature in the headspace and in the middle pathway. There is a slight reduction in air temperature along other pathways (positions 3-5-8-10). TD 2 provides more homogeneous cooling, particularly between the ACs in the first tray, which is consistent with the literature suggesting that an increase in the TOA enhances ventilation uniformity, and thus the products cooling (Delele et al., 2013). TD 2 outperforms the other designs, offering the advantage of achieving rapid cooling under lower pressure drop compared to TD 1.

For TD 3 when compring to TD 1, the presence of higher headspace above the ACs negatively impacts the cooling performance, resulting in significantly higher HCT and SECT values ($p \leq 0.05$). The maximum HCT reached 5.7 h (AC10), representing a 110% increase from the maximum HCT of TD 1 (AC16). The maximum SECT reached 15.4 h (AC10), which is a 106 % increase from the maximum SECT of TD 1 (AC16). This effect can be attributed to the reduced ventilation of the vertical walls of the ACs in TD 3: air short-circuits the load above the ACs and less air circulates in the pathways between the ACs. This leads to lower CHTC values (Nasser eddine et al., 2023) and higher air
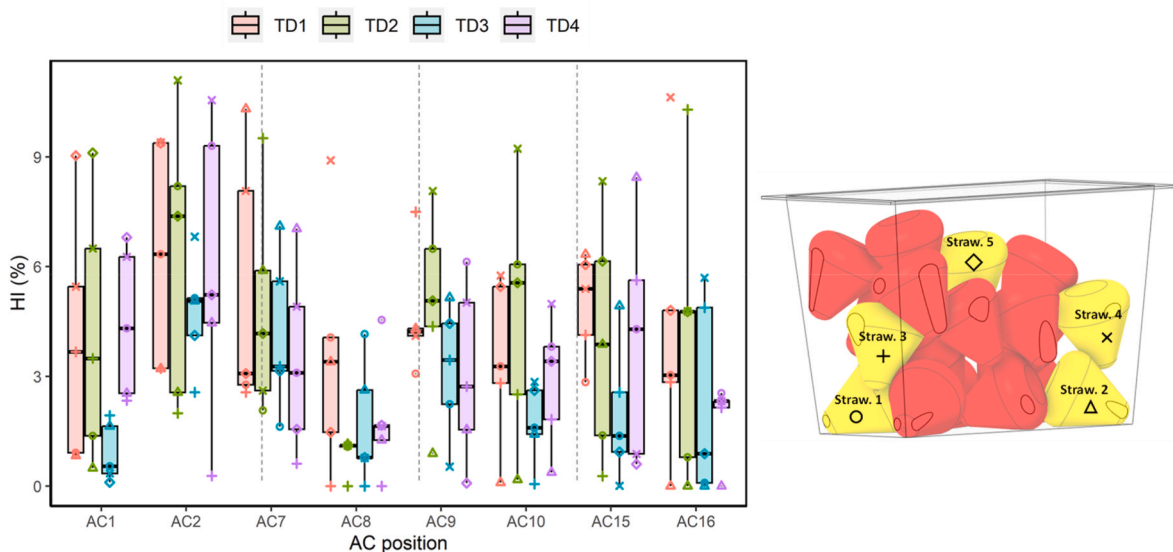

Fig. 9. Temperature heterogeneity of the 5 instrumented strawberries inside each AC (8 ACs in total) at the half-cooling time for 4 tray designs: 137 min for TD 1, 126 min for TD 2, 262 min for TD 3 and 197 min for TD 4; colors represent TD dessigns; symbol represent the strawberry position (airflow rate = 0.9 L s^{-1}.kg^{-1}).

temperature at 137 min in the positions at mid-height of the tray between the ACs (positions 1,2,3,4,5,6,7,8,9,10 in Fig. 8).

In TD 4, the addition of vent holes significantly improved HCT and SECT compared to TD 3, especially for the ACs placed in the first tray (maximum improvement of 60% in AC2 for HCT and SECT). No significant difference in HCT and SECT was observed for ACs 7,15 and 16. The additional vent holes allowed for more cold air penetration between the ACs and that can be seen in Fig. 8 by the high decrease of air temperature in the pathways separing ACs compared to TD 3 (positions 1-3-5). In comparison to TD 1 and TD 2, TD 4 shows also significantly higher HCT and SECT exluding for AC1 and AC2.

Fig. 9 displays the HI of 5 strawberries within 8 ACs in various tray designs. For TD 1, the average heterogeneity index was 5% and the maximum value of 11%, was reached in AC16. Adding vent holes in TD 2 didn't improve the HI with average and maximum values (respectively 4% and 11%) similar to the ones of TD 1. It's worth noting that TD 3 achieved the lowest heterogeneity (average 3%, maximum 7%) which can be attributed to the more homogeneous CHTC on the vertical walls in this configuration. Adding vent holes in TD 4 increased the HI inside the ACs (average 4%, maximum 11%). Consequently, the side CHTC heterogeneities found in our previous study (Nasser eddine et al., 2023) had a limited impact on strawberry temperature heterogeneities inside ACs.

3.3. Effect of the airflow rate

The influence of airflow rate on the cooling time of strawberries is depicted in Fig. 10. It is obvious that reducing the inlet velocity has a substantial impact on cooling times, as indicated by HCT and SECT. The maximum HCT increased significantly from 2.7 h for case 1 (condition often observed in FAC) to 6.4 h for case 2 (condition often observed in cold room), and SECT increased from 7.4 h to 16.2 h for AC16. These results are similar to those found in the literature (Castro et al., 2004; Defraeye et al., 2014; O'Sullivan et al., 2016). This can be attributed to the decreased velocities within the trays, affecting the CHTC of the ACs. Another contributing factor is observed when examining air temperatures after 137 min of cooling, as shown in Fig. 11. Here, it becomes obvious that the air experiences significant warming along the airflow, increasing from 5 °C at the inlet orifice to 14 °C at the outlet orifice at low flow rate. A similar warming trend is observed in the air pathways between the ACs. As a result, it is evident that the cooling heterogeneity between different AC positions has increased with a reduction in the airflow rate.

3.4. System energy consumption

Table 3 represents the influence of airflow rate and package design on ventilation energy consumption (FAC fans). For TD 1, decreasing the
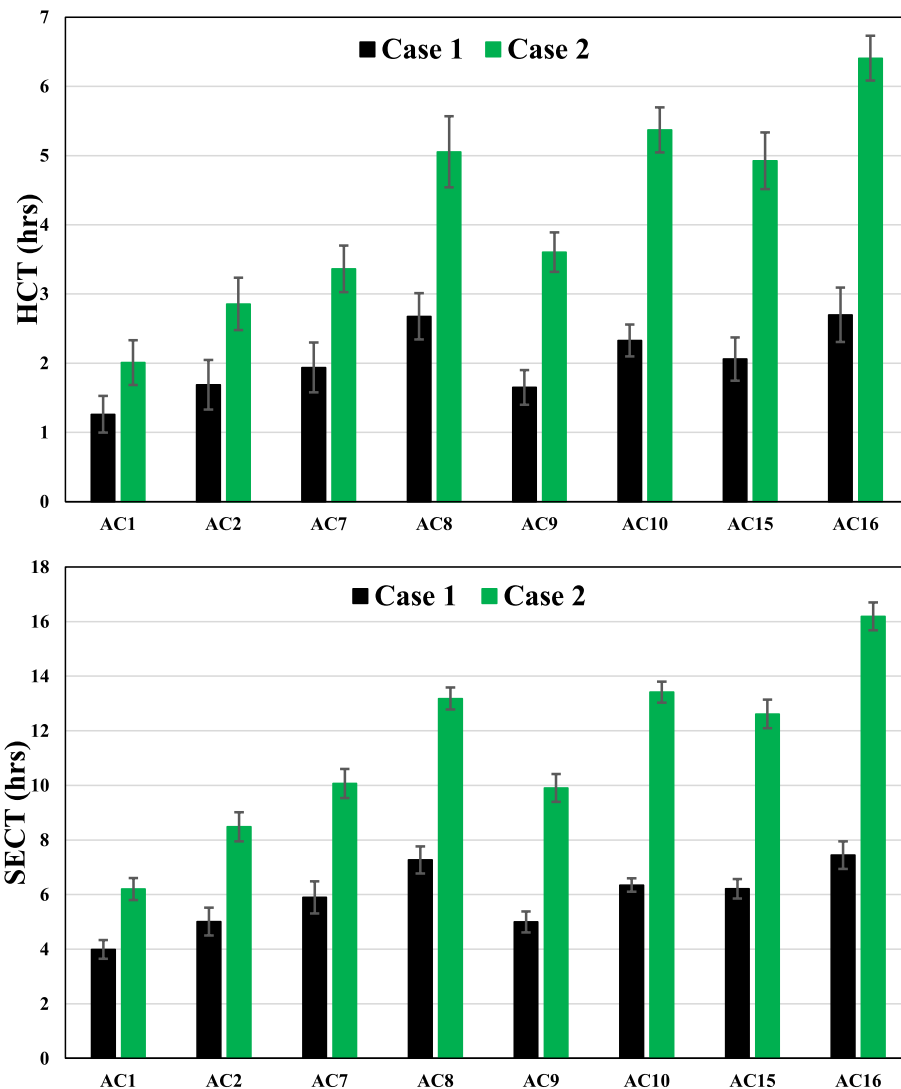

Fig. 10. HCT (hrs) and SECT (hrs) for TD 1 at two airflow rates, case 1: 0.9 L s^{-1}.kg^{-1}, case 2: 0.2 L s^{-1}.kg^{-1}.
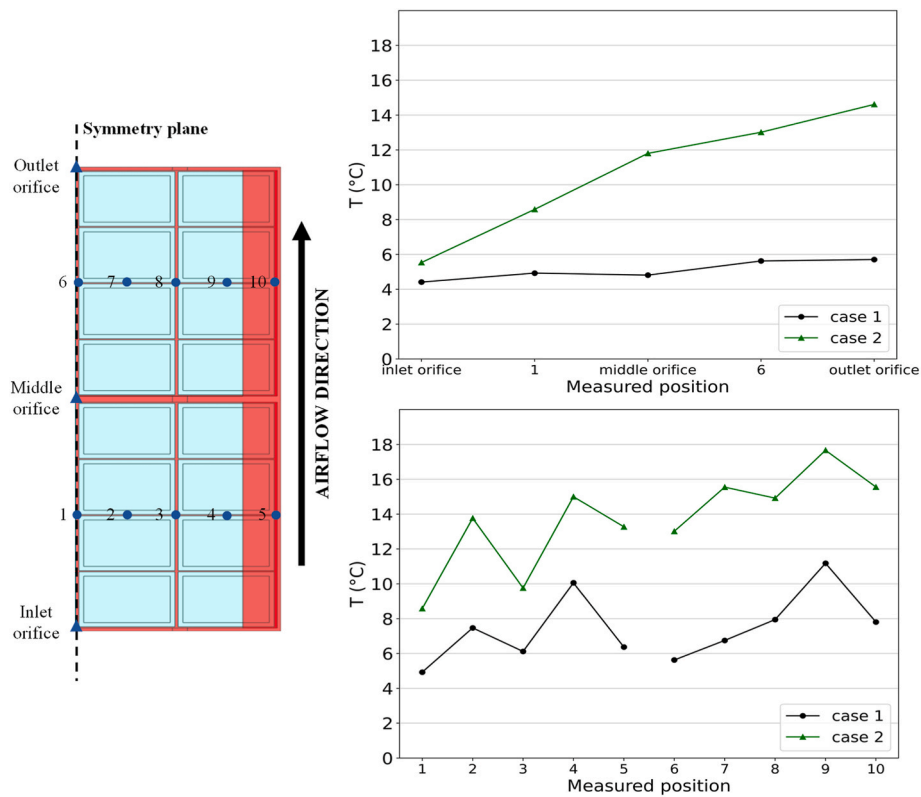
Fig. 11. Recorded air temperatures from various positions within the two trays (TD 1) after 137 min of cooling, with two cases distinguished by airflow rates: 0.9 L s⁻¹.kg⁻¹ and 0.2 L s⁻¹.kg⁻¹ for case 1 and case 2 respectively.

Table 3
System energy consumption for the different cases studied.

Tray design	Debit (L.s⁻¹. kg⁻¹)	Δp (Pa) ± measurement uncertainty	SECT_max (h)	P_comp (W)	E_FAC fan (W. h)	Energy consumption reduction compared to the reference case (%)
TD 1-case 1	0.9	10.5 ± 0.4	7.9	19.92	0.74	
TD 1-case 2	0.2	1.2 ± 0.3	16.8	9.37	0.04	94
TD 2	0.9	7.0 ± 0.4	7.9	19.92	0.49	33
TD 3	0.9	2.4 ± 0.3	15.7	10.06	0.33	55
TD 4	0.9	1.8 ± 0.3	12.2	12.94	0.19	74

airflow rate resulted in a reduced pressure drop from 10.5 to 1.2 Pa (Table 2). This lower pressure drop led to a 94 % decrease in energy requirements. Similar observations can be made when comparing different tray designs. Comparing TD 3 and TD 4 with TD 1 at the same airflow rate, there is a lower pressure drop and energy consumption with a larger headspace, but also slower cooling, which could impact the quality of strawberries. The relative P_{comp} is presented in Table 3, reflecting the design of the refrigerating process. It can be noticed that shorter cooling time requires higher P_{comp}, leading to larger refrigerating systems and higher investing costs.

It should be noted that a holistic approach to calculating energy consumption should consider not only the power usage of the FAC fans but also the power usage of the refrigeration unit taking into account all the loads within a cooling facility. For example, TD 1 and TD 2 demonstrated the fastest cooling time (SECT_max of 7.9 h). Using the same refrigerating system, these two designs could result in the lowest energy consumption of the others components of the refrigeration system (evaporator and condenser fans, control system, and pumps). This type of approach is well adapted to a cooling facility with pallets to ensure a realistic scenario and significant results. Such approach would provide a more accurate representation of the impact of package design on energy consumption.

Additionnaly, a multiparameter analysis is crucial, considering the quality of strawberries, logistics, costs for the different conditions and designs. This analysis can help identify a compromise to choose the optimal package design and operating conditions.

3.5. Relation between HCT and CHTC

Fig. 12 presents the HCT of strawberries (straw.5 in Fig. 3c) in all ACs in function of the external thermal resistance $R_{ext,j}$ (eq. (7)) for the different tray designs.

$$R_{ext,i} = \frac{1}{CHTC_{avg,i} \times S} \qquad (7)$$

where $CHTC_{avg,i}$ values were taken from our previous study (Nasser eddine et al., 2023) and S is the total surface area of an AC (m²). This equation shows that increasing CHTC (e.g. increasing airflow rate between cooling air and the walls of ACs) leads to decrease the external resistance, thus, cooling time decreases.

This figure shows a linear correlation between the R_{ext} and the HCT with a regression coefficient of 0.88. TD 3 with the lowest CHTC (Nasser
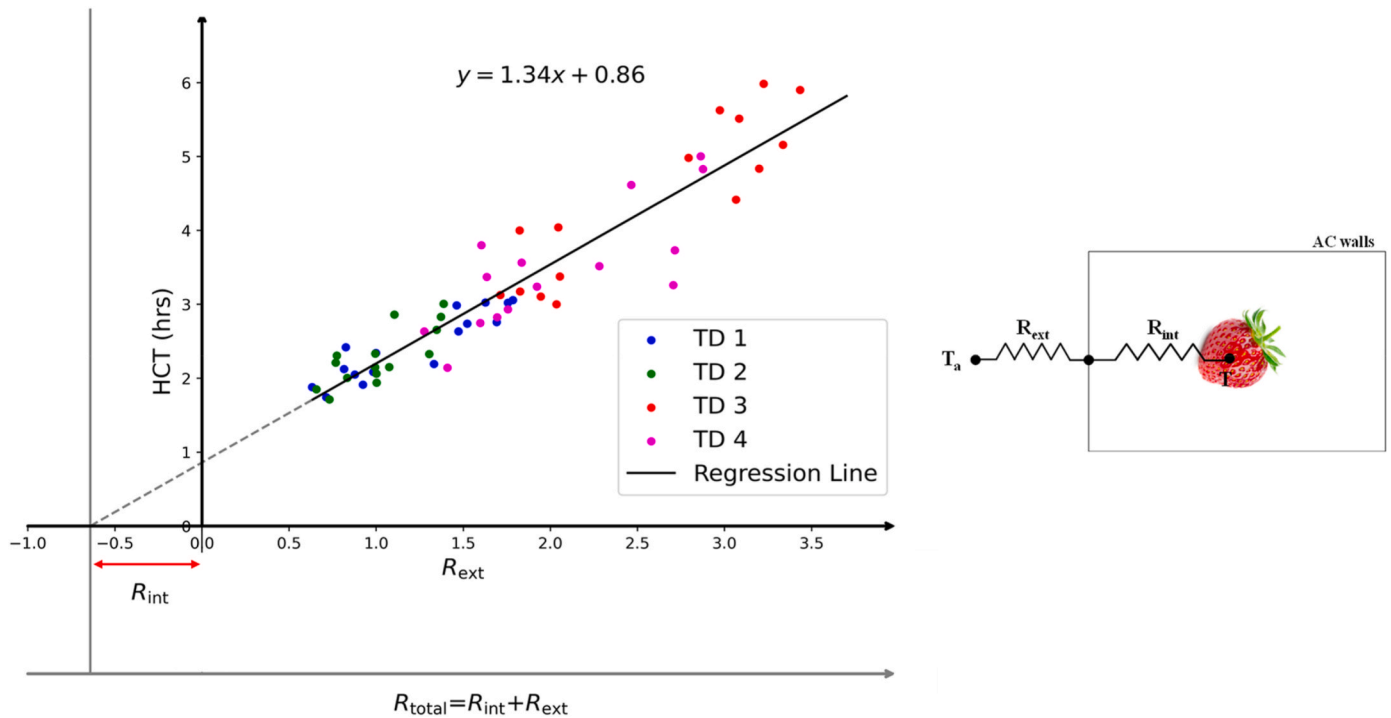
Fig. 12. HCT (hrs) of strawberry (Straw.5) in all ACs in function of the R_{ext} (K.W^{-1}).

eddine et al., 2023), exhibits the highest cooling time, while TD 1 and TD 2, with higher CHTC values, demonstrate shorter cooling times. As discussed previously, the airflow dynamics within the tray primarily influences the CHTC on the walls of the ACs and air temperature (in the air pathways between the ACs and in the headspace above them), thereby affecting the cooling behavior of the strawberries inside the ACs. This correlation provides valuable insights for researchers and operators in evaluating the performance of alteranive designs solely by experimental measurements or numerical calculation of the CHCT on the AC walls.

Extending the regression line in Fig. 12 enables the determination of the internal resistance R_{int} from the intersection with the x-axis. In this way, HCT can be considered as proportional to $R_{ext} + R_{int}$. This R_{int} involves natural convection inside the AC, air and strawberry thermal conductivites. R_{int} depends on the position of the strawberry inside the AC.

This relationship can be interpreted by a straightforward heat balance calculation. Eq (8) depicts the heat exchange between the cooling air and the load within the AC while the main simplifying assumption is that local air temperature is close to the set (upwind) temperature (T_a).

$$mCp\frac{dT}{dt} = \frac{T_a - T}{R_{ext} + R_{int}} \tag{8}$$

Exponential decaying function can be extracted from eq (8):

$$Y = \frac{T - T_a}{T_i - T_a} = e^{-\frac{t}{\tau}} \tag{9}$$

where the characteristic cooling time $\tau = mCp(R_{ext} + R_{int})$.

Y = 1/2 and 1/8 for HCT and SECT respectively.

The following equation can be derived from eq. (9):

$$t = mCp(R_{ext} + R_{int})\ln(Y) \tag{10}$$

Even if the assumptions of this simple model are questionable, this explains the direct (almost linear) relation between HCT and the two thermal resistances. It can be observed that the internal thermal resistance is weak compared to the external one for TD 4 but comparable for TD 1.

4. Conclusion

Experiments were conducted at laboratory scale under well-controlled conditions to monitor the temperature evolution of strawberries inside airtight clamshells (primary packaging) arranged within a tray (secondary packaging) during precooling (forced-air cooling). The study aimed to assess the influence of two facors: tray design (i.e. height of air headspace, additional vent holes in the current tray) and airflow rate, on cooling rates and temperature heterogeneities.

The finding indicated that there were minor cooling heterogeneities of product within the same ACs, regardless of their positions within the tray or the tray design (less than 11% of the difference between product temperature and upwind air temperature at HCT). However, significant hetergoneities were observed between the different AC positions within the tray.

This investigation highlights the critical importance of ensuring proper ventilation of the vertical walls of the ACs in order to ensure a fast cooling, revealing that TD 2, which includes additional vent holes, cools slightly better than TD 1 and exhibits lower ventilation energy consumption when working at the same airflow rate. On the other hand, TD 3, which have a larger headspace above the ACs, shows the slowest cooling rate due to the lack of ventilation of the vertical walls of the ACs. Interestingly, Tray Design 4, which combines the features of added orifices and higher headspace, shows an improved cooling rate over TD 3, though it doesn't quite match the efficiency of TD 2, and notably reduces the energy required for fan operation by 74%. The study also notes that reducing the airflow rate can significantly lower energy consumption for ventilation (FAC fans), but this comes at the expense of slower cooling rates, which could potentially compromise the quality of the product and result in higher consumption of some components of the refrigeration system.

A linear correlation was established between cooling time and thermal resistances. It reinforces the importance of airflow pattern in the cooling process via the convective heat transfer coefficient between air and clamshell walls.

The use of airtight clamshells to simulate heat transfer within MAP is a notable approach in this study. This method provided a controlled

representation of the heat transfer within the MAP and the surrounding air within the tray, enabling an analysis of the cooling performance of strawberries and studying the effect of different tray designs. Future research should investigate how different tray designs and the uneven cooling within the tray impact the quality of strawberries stored in MAP. This could be achieved through numerical simulations using a generic quality model or through experimental study using real strawberries to consider all factors within the MAP. Additionally, research should delve into mass transfer issues, such as the qualitative aspect (potential of condensation) and quantitative aspect (mass of condensed water), to fully understand these effects on product quality inside a non-ventilated package.

CRediT authorship contribution statement

Ahmad Nasser eddine: Writing – original draft, Visualization, Software, Methodology, Investigation, Formal analysis, Conceptualization. **Steven Duret:** Writing – review & editing, Visualization, Supervision, Methodology, Conceptualization. **Denis Flick:** Writing – review & editing, Visualization, Supervision, Methodology. **Onrawee Laguerre:** Writing – review & editing. **Ichrak Sdiri:** Investigation. **Jean Moureh:** Writing – review & editing, Supervision, Methodology, Conceptualization.

Declaration of competing interest

The authors declare that they have no known competing financial interests or personal relationships that could have appeared to influence the work reported in this paper.

Data availability

Data will be made available on request.

Acknowledgements

References

Agyeman, E.K.K., Duret, S., Flick, D., Laguerre, O., Moureh, J., 2023. Computational modelling of airflow and heat transfer during cooling of stacked tomatoes: optimal crate design. Energies 16 (4). https://doi.org/10.3390/en16042048.

Anderson, B.A., Sarkar, A., Thompson, J.F., Singh, R.P., 2004. Commercial-scale forced-air cooling of packaged strawberries. Transactions of the ASAE 47 (1), 183–190. https://doi.org/10.13031/2013.15846.

Berry, T.M., Defraeye, T., Nicolai, B.M., Opara, U.L., 2016. Multiparameter analysis of cooling efficiency of ventilated fruit cartons using CFD: impact of vent hole design and internal packaging. Food Bioprocess Technol. 9 (9), 1481–1493. https://doi.org/10.1007/s11947-016-1733-y.

Brosnan, T., Sun, D.-W., 2001. Precooling techniques and applications for horticultural products — a review. Int. J. Refrig. 24 (2), 154–170. https://doi.org/10.1016/s0140-7007(00)00017-7.

Castro, L.R.d., Vigneault, C., Cortez, L.A.B., 2004. Effect of container opening area on air distribution during precooling of horticultural produce. Transactions of the ASAE 47 (6), 2033–2038. https://doi.org/10.13031/2013.17792.

Defraeye, T., Cronje, P., Berry, T., Opara, U.L., East, A., Hertog, M., Verboven, P., Nicolai, B., 2015. Towards integrated performance evaluation of future packaging for fresh produce in the cold chain. Trends Food Sci. Technol. 44 (2), 201–225. https://doi.org/10.1016/j.tifs.2015.04.008.

Defraeye, T., Lambrecht, R., Delele, M.A., Tsige, A.A., Opara, U.L., Cronjé, P., Verboven, P., Nicolai, B., 2014. Forced-convective cooling of citrus fruit: cooling conditions and energy consumption in relation to package design. J. Food Eng. 121, 118–127. https://doi.org/10.1016/j.jfoodeng.2013.08.021.

Defraeye, T., Lambrecht, R., Tsige, A.A., Delele, M.A., Opara, U.L., Cronjé, P., Verboven, P., Nicolai, B., 2013. Forced-convective cooling of citrus fruit: package design. J. Food Eng. 118 (1), 8–18. https://doi.org/10.1016/j.jfoodeng.2013.03.026.

Dehghannya, J., Ngadi, M., Vigneault, C., 2010. Mathematical modeling procedures for airflow, heat and mass transfer during forced convection cooling of produce: a review. Food Eng. Rev. 2 (4), 227–243. https://doi.org/10.1007/s12393-010-9027-z.

Dehghannya, J., Ngadi, M., Vigneault, C., 2011. Mathematical modeling of airflow and heat transfer during forced convection cooling of produce considering various package vent areas. Food Control 22 (8), 1393–1399. https://doi.org/10.1016/j.foodcont.2011.02.019.

Delahaye, A., Salehy, Y., Derens-Bertheau, E., Duret, S., Adlouni, M.E., Merouani, A., Annibal, S., Mireur, M., Merendet, V., Hoang, H.-M., 2023. Strawberry supply chain: energy and environmental assessment from a field study and comparison of different packaging materials. Int. J. Refrig. 153, 78–89. https://doi.org/10.1016/j.ijrefrig.2023.06.011.

Delele, M.A., Ngcobo, M.E.K., Getahun, S.T., Chen, L., Mellmann, J., Opara, U.L., 2013. Studying airflow and heat transfer characteristics of a horticultural produce packaging system using a 3-D CFD model. Part II: effect of package design. Postharvest Biol. Technol. 86, 546–555. https://doi.org/10.1016/j.postharvbio.2013.08.015.

Ferrua, M.J., Singh, R.P., 2009. Modeling the forced-air cooling process of fresh strawberry packages, Part I: numerical model. Int. J. Refrig. 32 (2), 335–348. https://doi.org/10.1016/j.ijrefrig.2008.04.010.

Gruyters, W., Defraeye, T., Verboven, P., Berry, T., Ambaw, A., Opara, U.L., Nicolai, B., 2019. Reusable boxes for a beneficial apple cold chain: a precooling analysis. Int. J. Refrig. 106, 338–349. https://doi.org/10.1016/j.ijrefrig.2019.07.003.

Han, J.-W., Qian, J.-P., Zhao, C.-J., Yang, X.-T., Fan, B.-L., 2017. Mathematical modelling of cooling efficiency of ventilated packaging: integral performance evaluation. Int. J. Heat Mass Tran. 111, 386–397. https://doi.org/10.1016/j.ijheatmasstransfer.2017.04.015.

Han, J.-W., Zhao, C.-J., Qian, J.-P., Ruiz-Garcia, L., Zhang, X., 2018. Numerical modeling of forced-air cooling of palletized apple: integral evaluation of cooling efficiency. Int. J. Refrig. 89, 131–141. https://doi.org/10.1016/j.ijrefrig.2018.02.012.

Kumar, A., Kumar, R., Subudhi, S., 2023. Numerical modeling of forced-air pre-cooling of fruits and vegetables: a review. Int. J. Refrig. 145, 217–232. https://doi.org/10.1016/j.ijrefrig.2022.09.007.

Mercier, S., Brecht, J.K., Uysal, I., 2019. Commercial forced-air precooling of strawberries: a temperature distribution and correlation study. J. Food Eng. 242, 47–54. https://doi.org/10.1016/j.jfoodeng.2018.07.028.

Mukama, M., Ambaw, A., Berry, T.M., Opara, U.L., 2017. Energy usage of forced air precooling of pomegranate fruit inside ventilated cartons. J. Food Eng. 215, 126–133. https://doi.org/10.1016/j.jfoodeng.2017.07.024.

Nasser eddine, A., Duret, S., Flick, D., Moureh, J., 2023. Convective heat transfer characteristics within a multi-package during precooling. J. Food Eng. 359 https://doi.org/10.1016/j.jfoodeng.2023.111710.

Nasser Eddine, A., Duret, S., Moureh, J., 2022. Interactions between package design, airflow, heat and mass transfer, and logistics in cold chain facilities for horticultural products. Energies 15 (22). https://doi.org/10.3390/en15228659.

Ngcobo, M.E.K., Delele, M.A., Opara, U.L., Meyer, C.J., 2013. Performance of multi-packaging for table grapes based on airflow, cooling rates and fruit quality. J. Food Eng. 116 (2), 613–621. https://doi.org/10.1016/j.jfoodeng.2012.12.044.

O'Sullivan, J., Ferrua, M.J., Love, R., Verboven, P., Nicolaï, B., East, A., 2016. Modelling the forced-air cooling mechanisms and performance of polylined horticultural produce. Postharvest Biol. Technol. 120, 23–35. https://doi.org/10.1016/j.postharvbio.2016.05.008.

Pathare, P.B., Opara, U.L., Vigneault, C., Delele, M.A., Al-Said, F.A.-J., 2012. Design of packaging vents for cooling fresh horticultural produce. Food Bioprocess Technol. 5 (6), 2031–2045. https://doi.org/10.1007/s11947-012-0883-9.

Rashvand, M., Matera, A., Altieri, G., Genovese, F., Fadiji, T., Linus Opara, U., Mohamadifar, M.A., Feyissa, A.H., Carlo Di Renzo, G., 2023. Recent advances in the potential of modeling and simulation to assess the performance of modified atmosphere packaging (MAP) systems for the fresh agricultural product: challenges and development. Trends Food Sci. Technol. 136, 48–63. https://doi.org/10.1016/j.tifs.2023.04.012.

Sadashive Gowda, B., Narasimham, G.S.V.L., Krishna Murthy, M.V., 1997. Forced-air precooling of spherical foods in bulk: a parametric study. Int. J. Heat Fluid Flow 18 (6), 613–624. https://doi.org/10.1016/s0142-727x(97)00028-3.

Wang, D., Lai, Y., Jia, B., Chen, R., Hui, X., 2020. The optimal design and energy consumption analysis of forced air pre-cooling packaging system. Appl. Therm. Eng. 165 https://doi.org/10.1016/j.applthermaleng.2019.114592.

Wang, D., Lai, Y.H., Zhao, H.X., Jia, B.G., Wang, Q., Yang, X.Z., 2019. Numerical and experimental investigation on forced-air cooling of commercial packaged strawberries. Int. J. Food Eng. 15 (7).

Wu, W., Cronjé, P., Verboven, P., Defraeye, T., 2019. Unveiling how ventilated packaging design and cold chain scenarios affect the cooling kinetics and fruit quality for each single citrus fruit in an entire pallet. Food Packag. Shelf Life 21. https://doi.org/10.1016/j.fpsl.2019.100369.

Wu, W., Häller, P., Cronjé, P., Defraeye, T., 2018. Full-scale experiments in forced-air precoolers for citrus fruit: impact of packaging design and fruit size on cooling rate and heterogeneity. Biosyst. Eng. 169, 115–125. https://doi.org/10.1016/j.biosystemseng.2018.02.003.

Zhao, C.-J., Han, J.-W., Yang, X.-T., Qian, J.-P., Fan, B.-L., 2016. A review of computational fluid dynamics for forced-air cooling process. Appl. Energy 168, 314–331. https://doi.org/10.1016/j.apenergy.2016.01.101.